

See discussions, stats, and author profiles for this publication at: <https://www.researchgate.net/publication/47508927>

Supersonic Beams at High Particle Densities: Model Description beyond the Ideal Gas Approximation

ARTICLE in THE JOURNAL OF PHYSICAL CHEMISTRY A · OCTOBER 2010

Impact Factor: 2.69 · DOI: 10.1021/jp102855m · Source: PubMed

CITATIONS

9

READS

42

3 AUTHORS:



[Wolfgang Christen](#)
Humboldt-Universität zu Berlin

31 PUBLICATIONS 398 CITATIONS

[SEE PROFILE](#)



[Klaus Rademann](#)
Humboldt-Universität zu Berlin

110 PUBLICATIONS 1,750 CITATIONS

[SEE PROFILE](#)



[Uzi Even](#)
Tel Aviv University

176 PUBLICATIONS 5,367 CITATIONS

[SEE PROFILE](#)

Supersonic Beams at High Particle Densities: Model Description beyond the Ideal Gas Approximation[†]

Wolfgang Christen,^{*,†} Klaus Rademann,[†] and Uzi Even[‡]

Institut für Chemie, Humboldt-Universität zu Berlin, 12489 Berlin, Germany, and Sackler School of Chemistry, Tel Aviv University, 69978 Tel Aviv, Israel

Received: March 30, 2010; Revised Manuscript Received: July 8, 2010

Supersonic molecular beams constitute a very powerful technique in modern chemical physics. They offer several unique features such as a directed, collision-free flow of particles, very high luminosity, and an unsurpassed strong adiabatic cooling during the jet expansion. While it is generally recognized that their maximum flow velocity depends on the molecular weight and the temperature of the working fluid in the stagnation reservoir, not a lot is known on the effects of elevated particle densities. Frequently, the characteristics of supersonic beams are treated in diverse approximations of an ideal gas expansion. In these simplified model descriptions, the real gas character of fluid systems is ignored, although particle associations are responsible for fundamental processes such as the formation of clusters, both in the reservoir at increased densities and during the jet expansion.

In this contribution, the various assumptions of ideal gas treatments of supersonic beams and their shortcomings are reviewed. It is shown in detail that a straightforward thermodynamic approach considering the initial and final enthalpy is capable of characterizing the terminal mean beam velocity, even at the liquid–vapor phase boundary and the critical point. Fluid properties are obtained using the most accurate equations of state available at present. This procedure provides the opportunity to naturally include the dramatic effects of nonideal gas behavior for a large variety of fluid systems. Besides the prediction of the terminal flow velocity, thermodynamic models of isentropic jet expansions permit an estimate of the upper limit of the beam temperature and the amount of condensation in the beam. These descriptions can even be extended to include spinodal decomposition processes, thus providing a generally applicable tool for investigating the two-phase region of high supersaturations not easily accessible otherwise.

Introduction

On the basis of the experimental and theoretical foundations of molecular flow and effusion laid out by Knudsen a hundred years ago,^{1,2} studies of gases at low pressure have led to the first observation of collision-free streams of molecules by Dunoyer in 1911.³ The advancement and further development of these atomic and molecular beams to an extremely powerful experimental technique are primarily due to the dedication of Stern,^{4–7} who was awarded the Nobel Prize in physics in 1943 in part for his seminal contributions to this *molecular ray* method. Other milestones in this context were the theoretical design study of a supersonic beam source by Kantrowitz and Grey,⁸ the experimental realization of supersonic nozzle jet expansions by Becker and Bier,⁹ and not least the invention of pulsed jet expansions by Hagenau.¹⁰ Quite a substantial number of disciplines in chemistry, physics, and engineering could emerge and progress only due the availability of an intense, collimated flow of collision-free particles with a narrow velocity distribution. Until today supersonic molecular beams continue to constitute an extremely versatile and rather popular experimental tool in science and technology.^{11–14} They are of prime importance in both basic and applied research fields such as analytical chemistry, cluster science, heterogeneous catalysis,

optical spectroscopy, quantum physics, surface science, and thin film growth. Focusing on the applications, more fundamental aspects of the jet expansion of compressible fluids have not been investigated in great detail. Although the dynamic evolution of a supersonic flow is determined by the conservation of energy, mass, and momentum, these conservation laws need to be supplemented with an appropriate characterization of the material properties of the working fluid via a suitable equation of state (EOS). In the past, several attempts have been made to include real fluid properties in a description of the nozzle flow, e.g., by a consideration of the heat of condensation or by employing a van der Waals or Redlich–Kwong EOS.^{15–26} Still, in almost all publications of supersonic beams merely the isentropic expansion of an ideal gas into vacuum is considered. While the advantage of this approximation is simplicity, the ideal gas model description fails at elevated particle densities, i.e., in both low temperature and high pressure applications. This failure has been impressively confirmed in several intriguing observations of velocity distributions of supersonic jets of helium^{27–30} and hydrogen³¹ at cryogenic conditions, and of carbon dioxide at supercritical conditions.^{32,33} But even for rare gases at room temperature and modest stagnation pressures of 400–600 kPa, the mean flow velocity deviates from the ideal gas prediction, as has been demonstrated recently utilizing highly accurate time-of-flight measurements of supersonic beams of tagged metastable argon atoms.³⁴ Likewise, predictions and limitations of the classical nucleation theory for cluster formation have been addressed in numerous calculations and experiments.

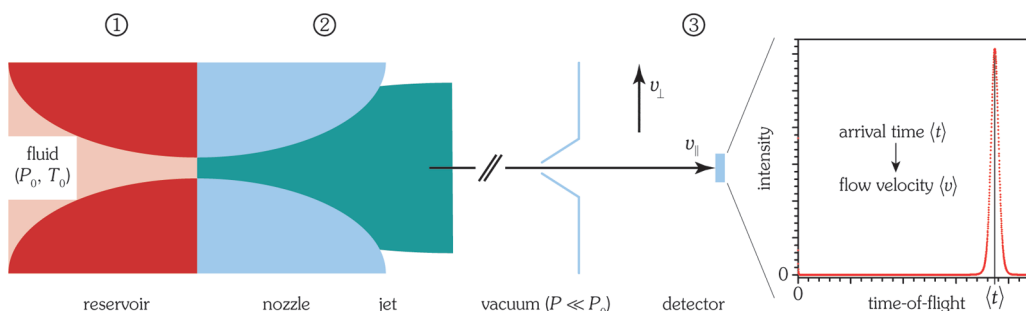
[†] Part of the “Klaus Müller-Dethlefs Festschrift”.

* To whom correspondence should be addressed, christen@wolfgang-christen.net.

[†] Humboldt-Universität zu Berlin.

[‡] Tel Aviv University.

SCHEME 1: Schematic Representation of a Macroscopic, Thermodynamic Description of an Effectively One-Dimensional Supersonic Jet Expansion of a Fluid System into a Vacuum^a



^a In the reservoir, the working fluid is characterized by two experimentally accessible properties, the source pressure P_0 and the source temperature T_0 . The assumptions of this model are (1) a thermal equilibrium between the working fluid and the stagnation reservoir, (2) no energy exchange between the effusing fluid and its environment (nozzle walls, background gas), a complete equalization of internal and kinetic particle energies, and (3) an on-axis detection of the undisturbed beam at a large distance. The asymptotic mean beam velocity $\langle v \rangle$ can be derived from time-of-flight spectra;⁶⁹ it is equivalent to the magnitude of the parallel velocity component $v_{||}$ on the symmetry axis.

Although it is common knowledge that both the size and the mass flux density of clusters rise sharply with an increasing source pressure and a decreasing stagnation temperature,^{35–37} empirical estimates and scaling laws have been established only for a restricted density range and a limited number of systems.^{38–48} Much of the work on real gas effects and condensation has focused on improving interaction potentials, particularly on quantum corrections motivated by the quest for the helium dimer, calculations of scattering cross sections and the associated collision integrals, and various approximations in the numerical solution of the Boltzmann transport equation.^{24,49–57} Although this microscopic approach permits the inclusion of nonequilibrium effects and yields useful information such as the spatial intensity distribution of the jet, it requires accurate intermolecular potentials. Particularly at the gas–liquid phase boundary and close to the critical point this condition may be difficult to accomplish. Moreover, the calculation of collision integrals requires extensive numeric effort and hence is not yet feasible at elevated particle densities. A generally applicable, macroscopic description may thus be useful to investigate the influence of real fluid properties on the terminal beam velocity and the intricate process of cluster formation. A major benefit of this approach is the straightforward applicability to a large number of fluid systems, including and beyond the rare gases.

After a concise review of the common assumptions and simplifications underlying a thermodynamic description of supersonic jet expansions, we present a facile yet consistent real fluid approach that is capable of overcoming most of the inconsistencies and errors occurring in the ideal gas treatments of supersonic molecular beams. In order to unequivocally demonstrate that the widely used ideal gas model is defective for any system at elevated pressures, we have chosen to study the isentropic jet expansion of the seemingly ideal rare gases. The thermodynamic quantities required by the suggested procedure are obtained numerically employing the most advanced equations of state currently available for He,⁵⁸ Ne,⁵⁹ Ar,⁶⁰ Kr,⁶¹ and Xe.⁶¹ Because these fluid models also serve as a reference for the US National Institute of Standards and Technology (NIST), this approach permits a reliable and very accurate calculation of thermodynamic properties. In addition, it provides access to a wide range of pressures and temperatures, including first and foremost the liquid–vapor phase boundary and the critical point. With estimated uncertainties of the relevant fluid properties of less than 1%, the thermodynamic approach presented here enables systematic benchmark studies of the influence of particle–particle interactions on the terminal flow

velocity of supersonic beams. In turn, the experimental determination of asymptotic flow velocities of supersonic beams as a function of source pressure and temperature facilitates the exploration of complex issues such as cluster formation and spinodal decomposition.

In this contribution, the five stable rare gases are used as a model system to illustrate the generic ideas and results of the suggested, very general procedure. The first section reviews the supersonic jet expansion in terms of a macroscopic description, and the next section describes the steps required to apply this practice to real fluids. In the following paragraph the effect of condensation on the terminal flow velocity is discussed in detail. The subsequent section treats the influence of the isothermal throttling coefficient and the Joule–Thomson coefficient on supersonic flow, while the last two parts introduce more advanced issues of an isentropic jet expansion. In a forthcoming contribution these theoretical predictions are compared with experimental time-of-flight spectra of tagged, metastable atom beams. Related studies are also in progress for molecular systems such as CO₂, C₂H₄, and C₃H₈.

Adiabatic Jet Expansions

Thermodynamic Description. The supersonic jet expansion of any fluid system into a vacuum is well described in a thermodynamic picture with the following conditions (see Scheme 1):

1. *Before the expansion*, the working fluid is in a complete thermodynamic equilibrium with the reservoir, hence permitting the assignment of a well-defined, uniform fluid pressure and temperature. This pivotal assumption can be accomplished to a high degree in state-of-the-art experiments, demanding a sufficiently high particle density within the stagnation reservoir and, most importantly, negligibly small temperature and pressure gradients.

2. *During the expansion*, no energy is exchanged between the effusing fluid and its environment. This supposition of an adiabatic process is very well approximated if particle–particle interactions dominate over particle–surface interactions and collisions with the background gas by many orders of magnitude; experimentally, it can be satisfied close to the symmetry axis of the emerging beam, high jet densities, and a sufficiently low background pressure in the vacuum chamber.

3. *After the expansion*, the undisturbed beam is interrogated on the symmetry axis at a large distance, where particle–particle collisions have ceased and a steady state is attained. Here, the

one-dimensional Maxwell–Boltzmann velocity distribution is effectively indistinguishable from a shifted Gaussian function. Hence the mean flow velocity of the beam is virtually identical with the most probable velocity and can be directly used to calculate the mean kinetic energy.

However, a macroscopic description using a uniform beam temperature implicitly assumes a complete equalization of internal and kinetic energies. This conjecture is more difficult to deal with in experiments; noncompliance is reflected in artifacts such as an incomplete relaxation of rotational or vibrational excitations^{49,62,63} or the appearance of a velocity difference between lighter and heavier species at too low particle densities.^{64–68}

For a pure substance, the conservation of energy then yields the following relation between the initial and the final state of a quasi-one-dimensional molecular beam

$$\begin{aligned}\langle E \rangle &= U_0 + P_0 V_0 + \frac{N_A m \langle v_0 \rangle^2}{2} \\ &= U_1 + P_1 V_1 + \frac{N_A m \langle v_1 \rangle^2}{2}\end{aligned}$$

In the absence of external fields, the average total molar energy $\langle E \rangle$ consists of the internal molar energy U , describing the random translational and internal motions of the particles, the pressure–volume work PV due to the change in molar volume V of the fluid occurring at a pressure P , and the kinetic energy $N_A m \langle v \rangle^2/2$ resulting from the center-of-mass motion at a mean velocity $\langle v \rangle$ of N_A particles each with a mass m . $N_A = 6.022 \times 10^{23} \text{ mol}^{-1}$ is the Avogadro constant, and the index 0 marks the thermodynamic state of the fluid within the reservoir, prior to expansion, while the index 1 is used to describe the ultimate properties of the supersonic beam at a large distance from the nozzle. Due to the macroscopic approach, the particle ensemble is characterized by bulk material properties.

Employing the definition of the enthalpy as the Legendre transform of the internal energy with respect to volume, $H \equiv U + PV$, a universal expression for the terminal flow velocity $\langle v_1 \rangle$ of the beam can be derived

$$\langle v_1 \rangle = \sqrt{\frac{2(H_0 - H_1)}{N_A m} + \langle v_0 \rangle^2}$$

Provided that the center-of-mass motion of the fluid within the reservoir can be neglected, i.e., $\langle v_0 \rangle \approx 0$, the following relation for the terminal mean flow velocity of the expanded jet is obtained

$$\langle v_1 \rangle = \sqrt{\frac{2(H_0 - H_1)}{N_A m}} \quad (1)$$

Pulsed beams with a short opening time of the valve may comply with this simplification because usually the fraction of particles leaving the stagnation reservoir in the course of the expansion process is small. In principle, it is also possible to approximate $\langle v_0 \rangle = 0$ using continuous beams.

In expression 1 the maximum of the flow velocity that is permitted by the conservation of the total molar energy $\langle E \rangle$ is achieved if the change of enthalpy, $\Delta H = H_0 - H_1$, is largest. Because the enthalpies of the condensed phase and the vapor

phase of a substance differ at least by the enthalpy of vaporization, $\Delta_v H$, the highest beam velocity is obtained if the expansion process is accompanied by a condensation of the working fluid, i.e., for $\Delta H \geq \Delta_v H$. Hence the terminal flow velocity $\langle v_1 \rangle$ of a supersonic jet is affected not only by the source pressure and temperature but first and foremost by the initial and final aggregation states. Because of the additional contribution of the condensation energy to the directed translational motion of a supersonic jet, a cold and condensed beam may be expected to be significantly faster than a cold but gaseous beam, assuming the very same thermodynamic state in the stagnation reservoir.

Occasionally the following expression for the maximum mean flow velocity $\langle v_{\max} \rangle$ of a supersonic beam is found in literature

$$\langle v_{\max} \rangle = \sqrt{\frac{2H_0}{N_A m}} \quad (2)$$

While at first glance eq 2 seems mathematically correct for a vanishingly small residual enthalpy H_1 , any thermodynamic energy value at a single state point is absolutely arbitrary as long as its reference state is not justified by physical reasons.⁷⁰ Consequently, an infinitesimally small value of H_1 as assumed in eq 2 is not necessarily a result of the jet expansion; it is almost exclusively due to the selection of the reference state. This rather intricate affair will be discussed in proper detail below. It is important to note, however, that eq 1 is not limited by any assumption of ideal gas properties. Accordingly it is valid for the thermodynamic treatment of every fluid system, i.e., the adiabatic jet expansion of gases, liquids, and supercritical fluids into a vacuum.

Approximations. Attempting to overcome the delicate issue of a reasonable reference state for the enthalpy, eq 1 typically is transformed further using the relation

$$C_P = \left(\frac{\partial H}{\partial T} \right)_P$$

Assuming that the isobaric molar heat capacity C_P itself depends neither on pressure nor on temperature, the change in enthalpy caused by the adiabatic jet expansion, $H_0 - H_1$, can be ascribed to a proportional change in temperature

$$H_0 - H_1 = C_P(T_0 - T_1) \quad (3)$$

Here T_0 denotes the fluid temperature in the stagnation reservoir and T_1 the temperature of the expanded jet. However, eq 3 turns out to be a severe simplification due to the large temperature changes occurring in a supersonic jet expansion. Therefore this relation is only valid for the model representation of an ideal gas, while for any real fluid it presents a fairly questionable approximation. Even the isobaric heat capacities of rare gases such as helium or argon easily vary by a factor of 4 at temperatures below 300 K.^{58,60} Moreover, the direct use of the isobaric heat capacity prohibits any reasonable description of first-order phase transitions.⁷¹ As a consequence, expansion conditions close to the liquid–vapor phase boundary or the critical point of the working fluid inevitably will result in enormous errors of the calculated mean flow velocities. Despite these serious concerns, the formula

$$\langle v_1 \rangle = \sqrt{\frac{2C_P(T_0 - T_1)}{N_A m}}$$

is found in literature with increasing regularity. Mathematically it results from the combination of eqs 1 and 3 but is only valid for an ideal gas.

Interestingly enough, this poor description can be considerably improved by the substitution $C_P = C_V + R$. C_V is the molar heat capacity at constant volume and $R = 8.314472 \text{ J/(mol K)}$ the gas constant. Here, too, the relation is valid only for an ideal gas, but introducing the heat capacity ratio $\gamma = C_P/C_V$, where the pressure- and temperature-induced variations in both heat capacities partially cancel each other, it becomes possible to avoid the direct occurrence of the molar isobaric heat capacity C_P via the replacement

$$C_P = \frac{\gamma}{\gamma - 1}R$$

Thus the asymptotic mean flow velocity in a supersonic jet expansion of an ideal gas can be expressed as

$$\langle v_1 \rangle = \sqrt{\frac{2R\gamma(T_0 - T_1)}{(\gamma - 1)N_A m}}$$

In the limiting case of a vanishingly small beam temperature, $T_1 \ll T_0$, the maximum terminal flow velocity is achieved

$$\langle v_{\max} \rangle = \sqrt{\frac{2R\gamma T_0}{(\gamma - 1)N_A m}} \quad (4)$$

It should be pointed out that the neglect of the beam temperature in eq 4 implicitly assigns a reference state. For an ideal monatomic gas, the heat capacities are constant, with $C_P = 5R/2$ and $C_V = 3R/2$. Correspondingly, the heat capacity ratio is constant, too, with $\gamma = 5/3$, and eq 4 can be further simplified to yield

$$\langle v_{\max} \rangle = \sqrt{\frac{5RT_0}{N_A m}} \quad (5)$$

In this well-known description of the adiabatic jet expansion of an ideal gas, the maximum terminal flow velocity is proportional to the square root of the source temperature and inversely proportional to the square root of the particle mass. In contrast, the velocity does not depend on the density or pressure in the stagnation reservoir or on any particle property.

Although eqs 2 and 5 originate from the very same thermodynamic description of a free jet expansion into a vacuum, they are equivalent merely in the hypothetical case of an ideal gas. For all real gases, liquids, and supercritical fluids, exclusively the general model employing real fluid enthalpies, eq 1 and—with a proper choice of a reference state—eq 2, may be used for an appropriate characterization of beam properties.

Real Fluid Properties

Presumably one major reason for the widespread misapplication of ideal gas descriptions of real fluid systems stems from

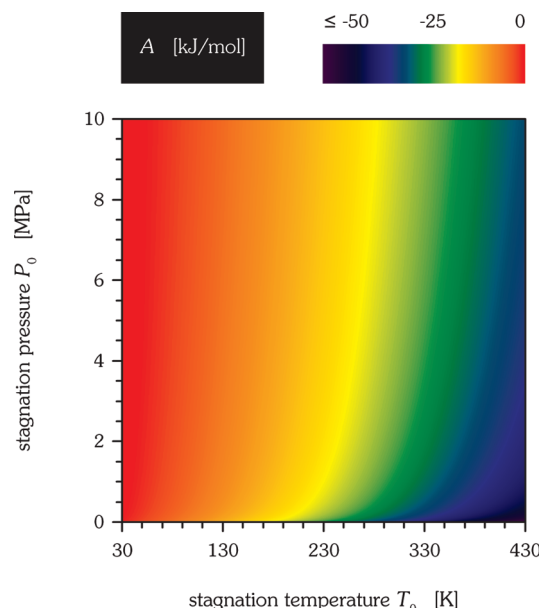


Figure 1. Graphical representation of the molar Helmholtz energy A of neon, obtained numerically from the most accurate EOS available at present,^{59,73} as a function of the experimentally accessible parameters stagnation pressure P_0 and stagnation temperature T_0 . The largest changes are observed for the transition from $P_0 = 0$ to $P_0 > 0$.

the temptation to use memorable numeric values for thermodynamic quantities such as $C_P = 5R/2$ or $\gamma = 5/3$. No analogous figure exists for the enthalpy. However, for many fluid systems, including all stable rare gases, dependable equations of state have been developed, permitting the straightforward computation of required material properties, e.g., the molar enthalpies H_0 and H_1 . In the following, our calculations of thermodynamic quantities are based on the most accurate equations of state available at present.^{58–61} These are empirical multiparameter descriptions of all experimental data available for a certain fluid.⁷² The compelling feature of this approach is the seamless applicability for all three fluid aggregation states, i.e., gaseous, liquid, and supercritical, including the gas–liquid phase transition and the critical point. The only restriction of these particular equations of state is that their lowest accessible temperature is given by the triple point temperature T_t . Hence they cannot describe solid clusters at ultralow temperatures. This, however, is not a limitation of the thermodynamic model.

Frequently the EOS is expressed in the molar Helmholtz energy A , which is a measure of the total available work. It is defined as the Legendre transform of the internal energy with respect to entropy, $A \equiv U - TS$, with S denoting the molar entropy. A graphic representation of the functional dependence of the Helmholtz energy A on the experimentally accessible parameters P_0 and T_0 is depicted in Figure 1 for neon over a wide range of stagnation conditions. Similar results are obtained for all other stable rare gases.

The practical value of an EOS explicit in the Helmholtz energy A is that all required thermodynamic properties can be assessed via a combination of derivatives of A . For example, the molar enthalpy H is deduced from the molar Helmholtz energy A using the relation

$$H = A + TS + PV$$

with

$$S = -\left(\frac{\partial A}{\partial T}\right)_V$$

and

$$P = -\left(\frac{\partial A}{\partial V}\right)_T$$

Similarly, numeric values for the heat capacity ratio γ in eq 4 can be obtained using the heat capacities C_P and C_V , together with the thermodynamic relations

$$C_V = \left(\frac{\partial U}{\partial T}\right)_V$$

and

$$U = A - \left(\frac{\partial A}{\partial T}\right)_V$$

Panels A and B of Figure 2 depict the entirely different functional dependencies of the molar enthalpy H and the heat capacity ratio γ on the experimentally accessible parameters stagnation pressure P_0 and stagnation temperature T_0 . The enthalpy exhibits a monotonous increase with temperature, and with the exception of the critical point and the vapor–liquid phase boundary, its changes are unobtrusive. This is in remarkable contrast to the heat capacity ratio featuring a pronounced maximum. Its parameter range reaches from the ideal gas limit at very low stagnation pressures and easily exceeds 10 times this value near the critical point. Panels C and D of Figure 2 illustrate reasons for the statement given above that the use of the heat capacity ratio γ helps in reducing the enormous errors found in a treatment involving the molar isobaric heat capacity: For C_P the apparent deviations from the ideal gas behavior are much more pronounced and extend to a much larger region around the critical point than for the heat capacity ratio.

Several relevant thermodynamic data of the stable rare gases as computed with the employed equations of state are summarized in Table 1.

Effects of Condensation

Since the first realization of cluster beams under high vacuum conditions,³⁵ it has been confirmed by a number of experiments that the mean flow velocity of supersonic beams may increase substantially with increasing stagnation pressure.^{17,41,74–77} While this observation has been routinely ascribed to the formation of clusters in the jet, the opposite behavior, a reduced flow velocity at higher pressures, has been reported as well.^{30,34,57,75,77} Obviously, an ideal gas description of the expansion process does not provide any pressure dependence of the terminal flow velocity, see eq 5, nor does it allow for any particle interactions that might form the physical basis for condensation processes in the jet or within the stagnation reservoir. It is thus mandatory to include these condensation phenomena in a real fluid treatment of supersonic jet expansions.

In general, i.e., for negative isothermal Joule–Thomson coefficients, $(\partial H/\partial P)_T < 0$, see below, the enthalpy of a fluid system decreases with increasing pressure due to enhanced associations between the particles. Accordingly, at higher source pressures the total initial energy of the working fluid that is available for a conversion into a directed translational motion

is reduced. For that reason the mean terminal flow velocity of a supersonic beam resulting from the adiabatic jet expansion into a vacuum is expected to decrease with increasing stagnation pressure. Simultaneously, however, the number of particle–particle interactions during the expansion process will rise at higher reservoir pressures. As a direct consequence, collisional cooling and nucleation in the evolving jet will become increasingly important. Because the enthalpy of the condensed phase of a substance is smaller than the enthalpy of its vapor phase at least by the enthalpy of vaporization, any cluster formation in the jet results in a diminished residual enthalpy. Indeed the degree of condensation in the expanding jet is the major factor determining the change of enthalpy. As the percentage of clusters in the jet increases, H_1 decreases relative to H_0 , yielding an increased terminal flow velocity, as can be seen readily from eq 1. In summary, both the initial aggregation state of the working fluid within the reservoir and the final aggregation state of the particles in the jet significantly affect the ultimate flow velocity of a supersonic beam.

In order to enable a numeric calculation of physically meaningful values for the asymptotic mean jet velocity $\langle v_1 \rangle$ using the real fluid description, eq 1, the topic of an adequate definition of the beam enthalpy, H_1 , needs to be tackled first. While the stagnation enthalpy H_0 directly arises as a result of the experimentally well-known source pressure and temperature, P_0 and T_0 , respectively, the terminal thermodynamic state of the beam is not easily accessible to experiments. As a consequence, the change of enthalpy that is needed for an application of eq 1 cannot be obtained without introducing further assumptions. For that reason in this model of an adiabatic jet expansion only limiting cases can be considered. The scenarios of most relevance are as follows: (I) A cold, fully condensed beam resulting from the jet expansion of a warm vapor; (II) a cold, completely gaseous beam resulting from the jet expansion of a warm vapor; (III) a cold, fully condensed beam resulting from the jet expansion of a warm liquid.

Obviously, the first case differs from (II) because it involves the additional release of condensation energy. Therefore, scenario (I) will yield the largest asymptotic flow velocity due to an extra contribution of the heat of condensation. The enthalpy of condensation is numerically equal to the enthalpy of vaporization, $\Delta_v H = H_v - H_l$, but with the opposite sign; the two indices v and l indicate the vapor and the liquid state of matter, respectively. The mean flow velocity $\langle v_1 \rangle$, resulting from the change of enthalpy during the expansion process, $\Delta H = H_0 - H_1$, is significantly larger if it also includes the enthalpy of vaporization, $\Delta_v H$. Because for any fluid system the largest value of the enthalpy of vaporization is encountered at the triple point, with $\Delta_v H_t = H_v(P_t, T_t) - H_l(P_t, T_t)$, an obvious estimate for the residual enthalpy of a cold, fully condensed jet is $H_1 = H_l(P_t, T_t)$. Thus, for a liquid beam the maximum of the mean terminal flow velocity of eq 1 can be phrased mathematically as

$$\langle v_{\max}(P_0, T_0) \rangle = \sqrt{\frac{2}{N_A m} [H_v(P_0, T_0) - H_l(P_t, T_t)]}$$

This definition of $\langle v_{\max} \rangle$ is equivalent to eq 2 provided that the enthalpy of the liquid composition of the fluid at the triple point is set to zero, $H_l(P_t, T_t) \equiv 0$. Customarily, however, enthalpies are given relative to the saturated liquid, e.g., at the normal boiling point. Although the latter choice of a standard state is recommended by NIST, this definition is arbitrary and not appropriate for a quantitative thermodynamic description of supersonic jet expansions.

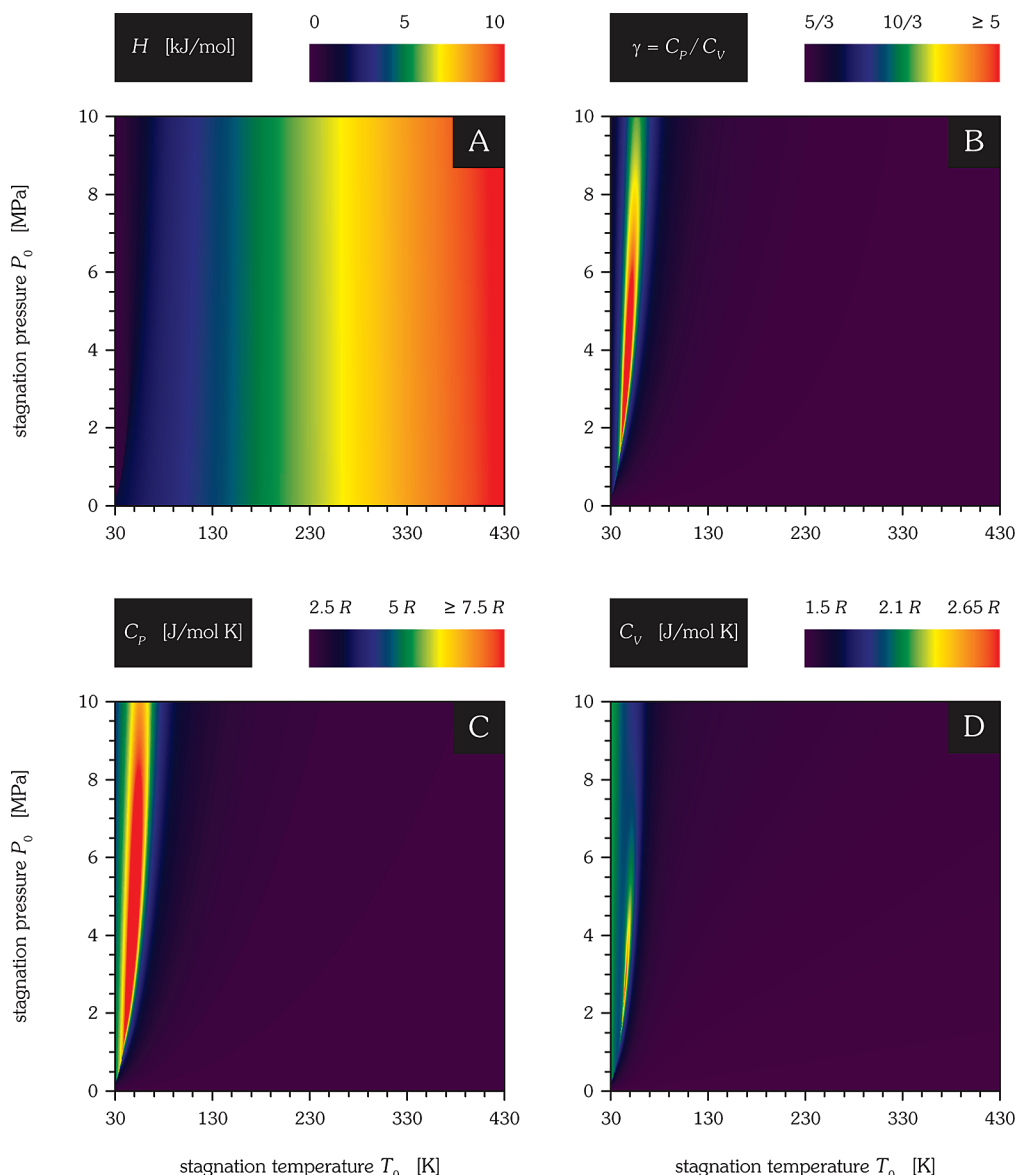


Figure 2. Visual comparison of the fundamentally different behavior of thermodynamic properties in the vicinity of the critical point. The data have been calculated employing the most accurate EOS currently available for neon,^{59,73} as a function of the experimentally accessible parameters stagnation pressure P_0 and stagnation temperature T_0 . For Ne, the critical point is located at a pressure of $P_c = 2.68$ MPa and a temperature of $T_c = 44.49$ K. (A) Molar enthalpy H , with numeric values relative to the saturated liquid at the normal boiling point at a temperature of 27.104 K, where $H \equiv 0$. (B) Heat capacity ratio $\gamma = C_p/C_v$. In general, the deviations from an ideal gas description ($\gamma = 5/3$) decrease with temperature and increase with pressure. They are most pronounced in the proximity of the critical point. (C) Molar isobaric heat capacity C_p . The parameter range where C_p exceeds the value of the ideal gas $5R/2$ by more than 300% is much larger than for the heat capacity ratio γ . (D) Molar isochoric heat capacity C_v . Deviations from the ideal gas value $3R/2$ do not exceed 80% even in the supercritical region. The estimated uncertainty of the EOS is 2% in heat capacities, except in the critical region.

TABLE 1: Numeric Values of Relevant Thermodynamic Properties for He,⁵⁸ Ne,⁵⁹ Ar,⁶⁰ Kr,⁶¹ and Xe,⁶¹ Calculated Using the Most Accurate Equations of State Available at Present: Triple Point Temperature T_t , Normal Boiling Point Temperature T_b , Critical Temperature T_c , Triple Point Pressure P_t , Critical Pressure P_c , and Vaporization Enthalpies $\Delta_v H_t$ and $\Delta_v H_b$ at the Triple Point and at the Normal Boiling Point, Respectively

	T_t (K)	T_b (K)	T_c (K)	P_t (kPa)	P_c (MPa)	$\Delta_v H_t$ (kJ/mol)	$\Delta_v H_b$ (kJ/mol)
⁴ He	2.18	4.23	5.20	4.86	0.227	0.093	0.083
Ne	24.56	27.10	44.49	43.37	2.679	1.778	1.730
Ar	83.81	87.30	150.69	68.89	4.863	6.540	6.437
Kr	115.78	119.73	209.48	73.53	5.525	9.084	8.971
Xe	161.41	165.05	289.73	81.77	5.842	12.657	12.550

This choice of an enthalpy reference state via the liquid part of the working fluid logically entails a finite flow velocity for the jet expansion of the gaseous portion—even at the triple point. Due to the enthalpy of vaporization, a gas in the stagnation reservoir may gain energy by condensation, and part of this

released energy can be converted into a directed center-of-mass motion during the expansion process. With the exception of helium (see Table 1), the heat of condensation exceeds the thermal energy at cryogenic temperatures by far. Hence the potential contribution of the enthalpy of vaporization $\Delta_v H$ on

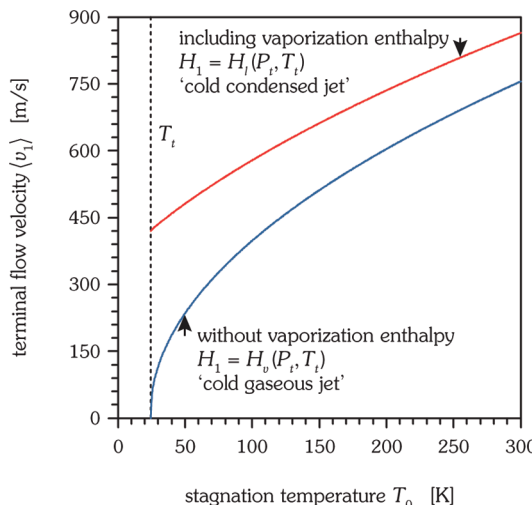


Figure 3. Mean terminal flow velocity $\langle v_1 \rangle$ of neon, calculated for a stagnation pressure of $P_0 = P_t = 43.37$ kPa according to eq 1: upper curve, the computation of $H_0 - H_1$ assumes a constant residual enthalpy of $H_1 = H_t(P_t, T_t)$, corresponding to scenario (I); lower curve, the computation uses a constant residual enthalpy of $H_1 = H_v(P_t, T_t)$, matching scenario (II). The two residual enthalpies differ by the enthalpy of vaporization at the triple point, $\Delta_v H_t = 1.778$ kJ/mol. The dotted line marks the triple point temperature of neon, $T_t = 24.56$ K.

the resulting terminal velocity of the molecular beam is particularly pronounced at low temperatures. This conclusion is illustrated in the upper (red) curve of Figure 3, depicting the maximum flow velocity of neon, calculated via eq 1 for a residual enthalpy of the beam $H_1 = H_t(P_t, T_t)$. At the given triple point pressure, the working fluid in the reservoir will be present in its vapor phase at temperatures $T_0 \geq T_t$. Exactly at the triple point, a fraction of the fluid will be liquid. The lower (blue) curve of Figure 3 depicts the mean terminal flow velocity of neon if the residual enthalpy of the beam is chosen to reflect a cold gas without any condensation, i.e., $H_1 = H_v(P_t, T_t)$. Hence this curve corresponds to the second case study (II) and demonstrates that the terminal flow velocity obtained in a real fluid description of the adiabatic jet expansion approaches zero at the minimum possible fluid temperature of $T_0 = T_t$. This is in marked contrast to the ideal gas description; see Figure 4 for a direct comparison. Even though the visual appearance of the enthalpy presentation seems to closely resemble the temperature dependence of an ideal gas jet expansion, i.e., $\langle v_{\max} \rangle \propto T_0^{1/2}$, and indeed can be very well approximated by a square root function, there is a fundamental disparity between the two apparently similar functional behaviors. Only at very high source temperatures and zero stagnation pressure both curves converge, whereas the temperature scales are offset by the triple point temperature. At the chosen source pressure of $P_0 = P_t$ and for temperatures below the triple point, the system is present in a solid phase; hence no jet expansion at all is possible. Yet this seemingly trivial fact—besides numerous others as outlined above—is completely ignored in the ideal gas picture.

Thus far, two limiting cases of the terminal flow velocity $\langle v_1 \rangle$ of a supersonic beam as specified by eq 1 have been considered, where the expansion of a vapor was either assumed to result in a cold and completely liquefied jet with a residual enthalpy of $H_1 = H_t(P_t, T_t)$ or to result in a cold but entirely gaseous jet, represented by a beam enthalpy of $H_1 = H_v(P_t, T_t)$. In practice, even a terminal solid state might be realized⁷⁸ and common source conditions will yield supersonic beams in between these extreme cases. Most importantly, with the

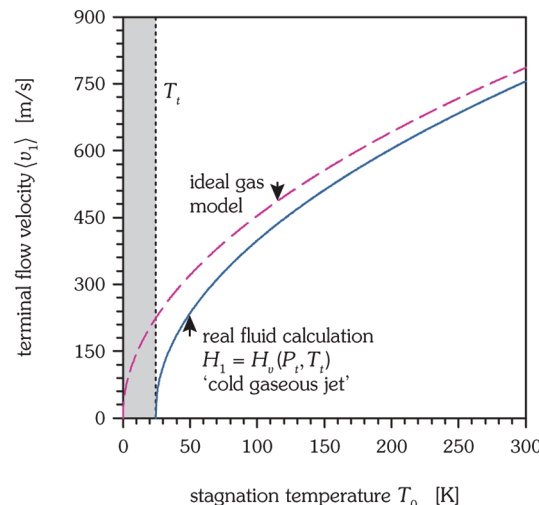


Figure 4. Mean terminal flow velocity $\langle v_1 \rangle$ of neon, calculated for a source pressure of $P_0 = P_t = 43.37$ kPa: upper curve, ideal gas model according to eq 5; lower curve, real fluid description according to eq 1, using a constant residual enthalpy of $H_1 = H_v(P_t, T_t)$, representing a noncondensed beam. The dotted line marks the triple point temperature of neon, $T_t = 24.56$ K. At the given source pressure, the shaded region to the left of the triple point temperature is not accessible in molecular beam expansions; this fact is disregarded in an ideal gas description.

assumption of an adiabatic jet expansion the overall pressure and temperature dependence of the mean beam velocity can be predicted, including the dramatic changes occurring at the liquid–vapor phase boundary.

Joule–Thomson and Throttling Coefficients

The dramatic influence of source pressure P_0 on the mean terminal flow velocity $\langle v_1 \rangle$ of a supersonic jet at a constant stagnation temperature T_0 is depicted in Figure 5 for helium and neon. These computations reveal a couple of interesting observations: At very low stagnation temperatures, a distinct minimum in the mean flow velocity is encountered. It is determined by the root of the isothermal throttling coefficient

$$\delta_T = \left(\frac{\partial H}{\partial P} \right)_T = 0$$

At increasingly higher stagnation temperatures, this minimum in the terminal flow velocity gets broader and less pronounced; its position shifts with pressure, see Figure 6. Above the inversion temperature the terminal flow velocity monotonously increases with pressure. The inversion temperature T_i of a real gas is defined via the root of the Joule–Thomson coefficient

$$\delta_H = \left(\frac{\partial T}{\partial P} \right)_H = 0$$

For helium at zero pressure, a value of $T_i = 38.92$ K is obtained. The only other rare gas with an inversion temperature below room temperature is neon with $T_i = 220.53$ K. For argon, this value already reaches $T_i = 763.31$ K and thus will be rarely relevant in experiments. The corresponding values for krypton and xenon exceed 1000 K and hence the range of applicability of the respective EOS. For helium, the minimum of the flow velocity at its critical temperature is encountered at a stagnation pressure of 412 kPa. For the other rare gases this minimum

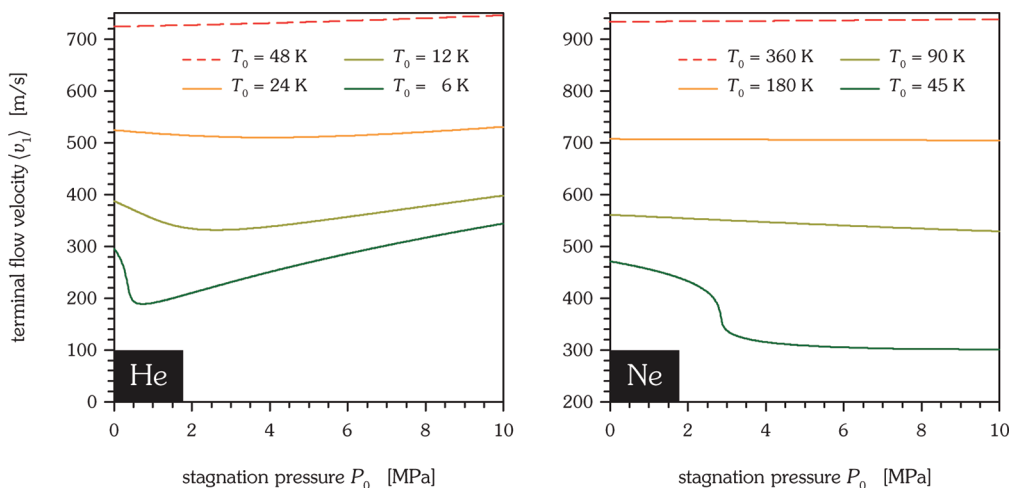


Figure 5. Mean terminal flow velocities $\langle v_1 \rangle$ of helium and neon at four characteristic stagnation temperatures T_0 , assuming a cold, fully condensed jet with a constant residual enthalpy of $H_1 = H_i(P_t, T_i)$, corresponding to scenario (I). In marked contrast, the flow velocities do not depend on pressure in an ideal gas description: here, for helium at the four source temperatures of $T_0 = 6, 12, 24$, and 48 K the values are $\langle v_1 \rangle = 249.6, 353.0, 499.3$, and 706.1 ms $^{-1}$, respectively. For neon, the corresponding numbers are $\langle v_1 \rangle = 304.5, 430.6, 609.0$, and 861.2 ms $^{-1}$ at the source temperatures of $T_0 = 45, 90, 180$, and 360 K.

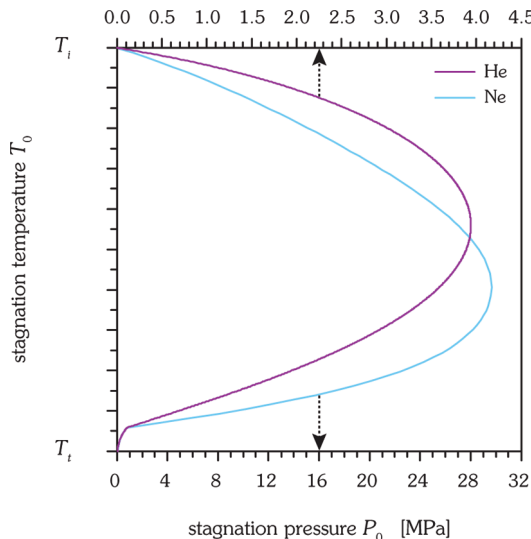


Figure 6. Pressure and temperature dependence of the minimum terminal flow velocity of helium and neon as defined by the isothermal throttling coefficient δ_T . The temperature axis scale ranges from the triple point temperature, T_t , up to the Joule–Thomson inversion temperature, T_i .

occurs at much higher pressures, for neon at 9.67 MPa, for argon at 19.09 MPa, for krypton at 21.97 MPa, and for xenon at 23.45 MPa. The direct comparison of the five stable rare gases is depicted in Figure 7.

In summary, at stagnation temperatures above the Joule–Thomson inversion temperature, the mean flow velocity increases with pressure, while at source temperatures $T_0 < T_i$ this behavior depends on the isothermal throttling coefficient.

Isentropic Jet Expansions

The two boundary values of zero and full condensation of the cold jet that have been described so far permit a discussion of the pressure and temperature dependence of the mean asymptotic flow velocity of supersonic beams. Nevertheless, in this very general thermodynamic picture the terminal beam temperature T_1 has been assumed to always equal the triple point temperature and not to depend on the actual stagnation conditions, P_0 and T_0 . In this respect, more information seems to be

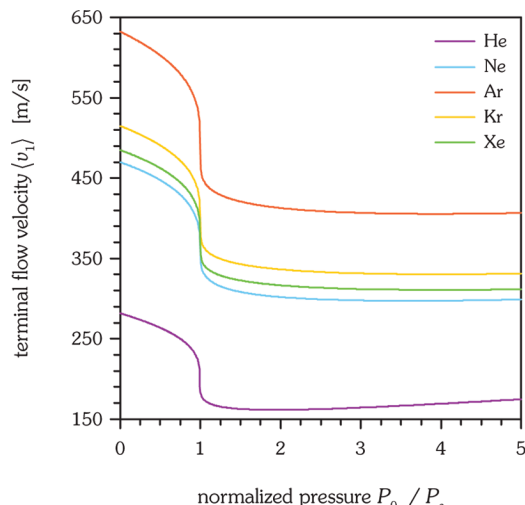


Figure 7. Mean terminal flow velocity $\langle v_1 \rangle$ of the five stable rare gases as a function of stagnation pressure. In order to facilitate a direct comparison, the source temperature T_0 has been chosen as the critical temperature T_c of the respective substance, and the source pressure P_0 has been normalized by the respective critical pressure, P_c . A constant residual enthalpy of $H_1 = H_i(P_t, T_i)$ has been assumed.

available that possibly could be incorporated into a refined model in order to reduce the substantial bandwidth of the predicted velocity values. For example, at elevated source temperatures and very low stagnation pressures no condensation is expected to occur during the jet expansion; accordingly, the velocity limit given by a fully condensed jet, scenario (I), appears to be of little practical relevance in this particular case, where one would intuitively apply scenario (II). A similar argument holds for the lower velocity limit in the case of strong cluster formation. Therefore, a more accurate estimate of the actual amount of condensation is required, in between the extreme cases of 0% and 100%. Here, the additional supposition of an isentropic expansion process might prove advantageous. While frequently adiabatic and isentropic jet expansions are put on a level, the latter process requires the additional assumption of reversibility, i.e., the lack of any dissipative mechanisms such as shock waves. The distinct advantage of modeling an isentropic jet expansion is the fact that in this case the residual enthalpy of the beam, H_1 , can be evaluated as a function of the stagnation conditions

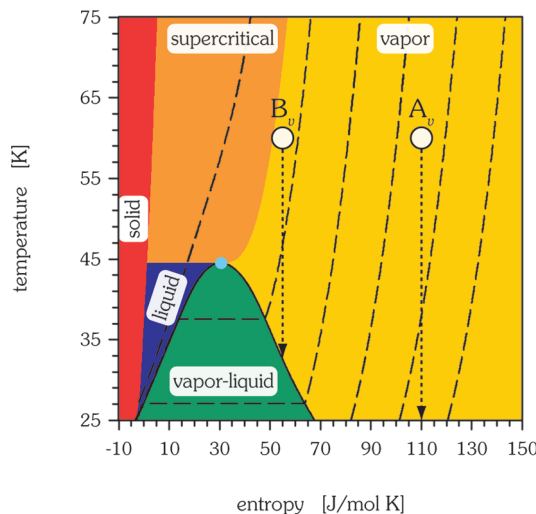


Figure 8. T - S phase diagram of Ne, calculated with the most accurate EOS available at present.^{59,73} The critical point is located at a temperature of $T_c = 44.49$ K and a molar entropy of $S_c = 30.76$ J/(mol K). The numeric values of the entropy are given relative to the normal boiling point, at a temperature of $T_b = 27.10$ K. The solid line enclosing the two-phase region marks the binodal curve; the dashed lines represent isobars of $P_0 = 0.1$ kPa, $P_0 = 1.0$ kPa, $P_0 = 10.0$ kPa, $P_0 = 0.1$ MPa, $P_0 = 1.0$ MPa, and $P_0 = 10.0$ MPa (from right to left). The dotted arrows originating from the state points A_v and B_v illustrate isentropic expansions starting from a gaseous aggregation state at a source temperature of $T_0 = 60.0$ K.

and the final beam temperature, T_1 . This characteristic can be best visualized in a temperature–entropy phase diagram of the working fluid as is pictured in Figure 8. One obvious benefit of this T – S representation is that isentropic processes are visualized as simple vertical trajectories; what is even more advantageous is the visibility of the two-phase region where condensation may take place. Supersonic expansions which originate in the vapor phase at a very low source pressure, equivalent to a comparatively large stagnation entropy S_0 , will not reach this region. The expansion path starting from the thermodynamic state A_v in Figure 8 illustrates such an isentropic trajectory. Hence, for sufficiently low stagnation pressures it is incidental from this phase diagram to expect a strictly gaseous beam; this is irrespective of the initial reservoir temperature. Provided that the precondition of ample particle–particle collisions during the jet expansion is fulfilled to allow for an equilibration of the internal and kinetic energies of all particles, very low beam temperatures T_1 might be expected in these cases.

In contrast, supersonic jet expansions which originate at somewhat elevated source pressures will arrive at the saturation curve, as is illustrated in Figure 8 by the vertical trajectory starting at the vapor state B_v . Thermodynamically, condensation is feasible at the gas–liquid phase boundary. Accordingly, isentropic expansions reaching the binodal line might be expected to yield both uncondensed particles and condensed species such as clusters and droplets. In this case, the ultimate beam temperature will not be as low as without cluster formation due to the release of condensation energy. As a consequence, the upper limit of the beam temperature T_1 can be characterized by the saturation temperature of the fluid at the stagnation entropy, $T_{\text{sat}}(S_0)$. Arriving at the saturation curve, the isentropic expansion may continue until a substantial degree of supersaturation is reached and rapid condensation sets in. In the continuum thermodynamic point of view this phase separation will occur at the latest when for the same temperature and total volume any combination of a saturated liquid and a vapor have

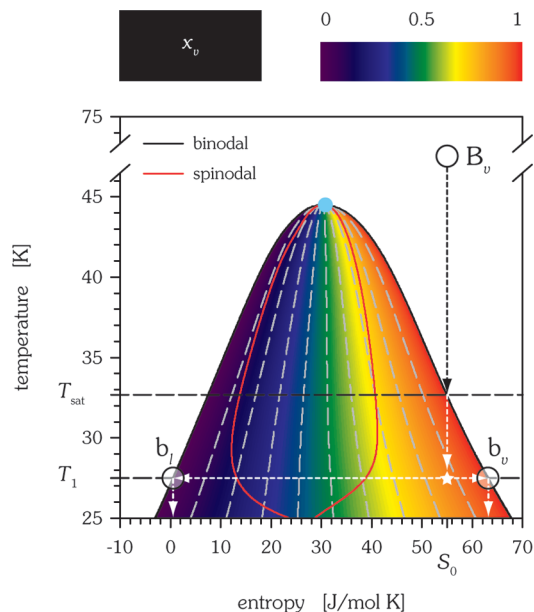


Figure 9. T - S phase diagram of neon, showing the two-phase region in detail. The vapor quality, x_v , is indicated by the color scale and the gray dashed lines of constant vapor quality. The black solid line marks the vapor–liquid phase boundary, and the red solid line the spinodal curve. The black dotted arrow illustrates an isentropic expansion path originating from the state point B_v , located in the vapor phase, to the saturation line at a temperature $T_{\text{sat}}(S_0)$. From here it may further continue into the two-phase region down to a temperature T_1 where rapid nucleation of a large number of particles sets in; this state point is indicated by a white star. The subsequent isothermal phase separation will yield condensed and noncondensed species at the state points b_l and b_v . Consequently, real flows with significant condensation will not be fully isentropic because the trajectory will include isothermal processes and move to different entropies in the T - S diagram.

a lower Helmholtz energy than the homogeneous phase. This condition is met at the spinodal line and can be characterized by the equation

$$\left(\frac{\partial^2 A}{\partial V^2}\right)_T = 0$$

While the condensation of a vapor at low supersaturations, close to the thermodynamic phase equilibrium, is an activated and hence comparatively slow process which requires the formation of critical nuclei, the energetic barrier to a phase separation vanishes at the spinodal limit. Accordingly, at the spinodal line the homogeneous phase will decompose all at once. However, this sharp stability criterion as given by the macroscopic thermodynamic approach is somewhat blurred in a more rigorous, microscopic theory.⁷⁹ After the phase separation the newly formed clusters and droplets may grow isothermally until the saturation curve is reached. This process is schematically illustrated in Figure 9 by the white horizontal arrows pointing toward the state points b_v and b_l . The relative intensities of the gaseous and the condensed portion of the beam are characterized by the vapor quality at the initial entropy S_0 and the beam temperature T_1 , $x_v(T_1, S_0)$. As an important result, the additional assumption of an isentropic expansion process permits estimation of the relevance of cluster formation for a given thermodynamic state of the working fluid, (P_0, T_0), via the calculation of the stagnation entropy, $S_0(P_0, T_0)$. This entropy then specifies if, and at what temperature, the two-phase region will be reached. The vapor and the liquid regions of the jet are

characterized by two distinct residual enthalpies, H_{1v} and H_{1l} , respectively, differing by the enthalpy of vaporization. Neglecting solidification, the residual enthalpy of the beam is given by $H_1 = (1 - x_v)H_{1l} + x_vH_{1v}$, and for the constraint of a dissipation-free jet expansion, eq 1 may be generalized by introducing the two residual enthalpies of the liquid and the vapor fraction of the beam

$$\langle v_1 \rangle = \sqrt{\frac{2[H_0 - (1 - x_v)H_{1l} - x_vH_{1v}]}{N_A m}} \quad (6)$$

In order to reasonably assess the mean terminal flow velocity of the beam, the following scenarios are considered to provide valuable insight: (i) the expansion ceases already at the binodal line, this case results in the lower velocity limit; (ii) the expansion ceases at the spinodal line, where phase separation of the metastable fluid occurs; (iii) the expansion continues as an isentropic process, this case results in the upper velocity limit. These isentropic case studies can be considered the equivalent of the limiting cases of the adiabatic model description; the major improvements are 2-fold: first, the end state H_1 does depend on the initial stagnation pressure via the stagnation entropy $S_0(P_0, T_0)$; second, the calculation of the residual enthalpy relies on a more gradual consideration of condensation than in the adiabatic case. In the following isentropic scenarios, if no binodal line exists for a given stagnation entropy, as is the case at very low source pressures, the expansion is assumed to continue until the triple point temperature is reached. In general, the relevance of the two case studies (i) and (ii), binodal versus spinodal, is not at par, because for kinetic reasons a condensation will not set in until high supersaturations are attained, i.e., at temperatures well below the saturation curve. These considerations are brought together in Figure 10, depicting computational results for the isentropic jet expansion of neon at a stagnation temperature of $T_0 = 60$ K, as a function of the source pressure, P_0 . These computations reveal quite a few interesting observations: First, the stagnation enthalpy H_0 decreases with increasing pressure due to the enhanced particle associations in the reservoir, as can be seen in Figure 10A. Second, above a stagnation pressure of $P_0 = 0.443$ MPa an isentropic jet expansion of neon originating at a source temperature of $T_0 = 60$ K will arrive at the vapor–liquid region. Accordingly, partial condensation of the gaseous jet may occur, with varying contributions of the vapor and liquid fraction to the residual enthalpy of the beam. Both scenarios for the terminal thermodynamic state, the binodal (light blue curve) as well as the spinodal (dark blue curve), are provided in the figure. In general, the residual enthalpy decreases with increasing pressure, too. This observation may change only when the isentropic expansion path hits the stability limits of the two-phase region, resulting in an initially increasing beam temperature (Figure 10B). This behavior is usually rationalized by the release of heat of condensation. Due to the higher beam temperature, the residual enthalpy is larger as well. However, because the condensed fraction of the beam is increasing with pressure, ultimately the residual enthalpy will decline again. Intriguingly, at elevated pressures both case studies yield virtually the same numeric values for the residual enthalpy of the beam.

The consequence of the net change in enthalpy on the terminal flow velocity is summarized in Figure 11. Compared with the maximum boundary of an adiabatic jet expansion obtained for a cold, fully condensed beam with a constant residual enthalpy of $H_1 = H(P_t, T_t)$, isentropic flow velocities are consistently

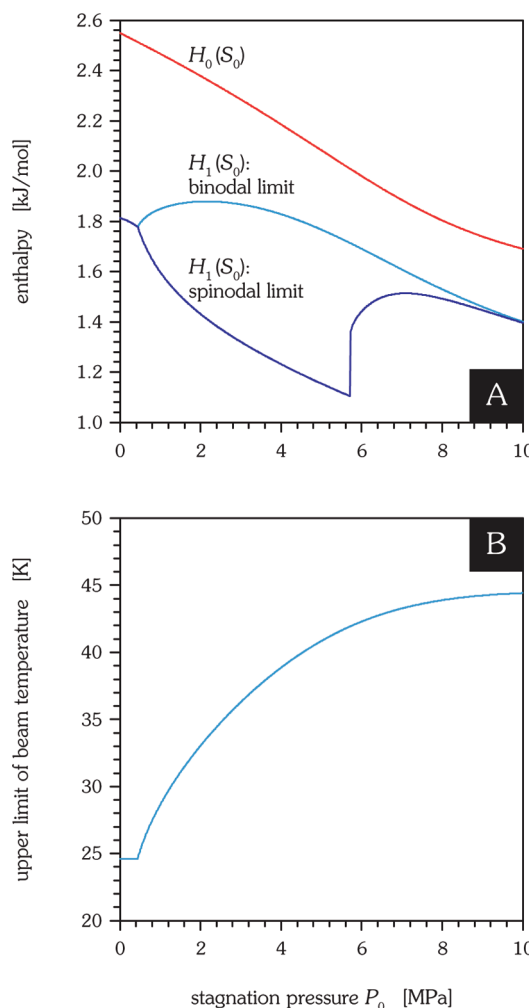


Figure 10. Properties of a supersonic beam of Ne at a source temperature of $T_0 = 60.0$ K. (A) Stagnation enthalpy H_0 and possible residual enthalpies of the beam $H_1(S_0)$, corresponding to scenarios (i) and (ii). Enthalpy values are given with respect to the enthalpy of the liquid at the triple point temperature. (B) Estimate of the upper limit of the beam temperature via the binodal line, $T_{\text{sat}}(S_0)$. At lower pressures, where the two-phase region is not reached, temperature values are given by the triple point temperature T_t .

smaller. They are, however, very close to the adiabatic case study of a cold gaseous beam, characterized by $H_1 = H_v(P_t, T_t)$; see Figure 3. Moreover, even at a stagnation pressure of only 1 kPa a gaseous jet as calculated with eq 6 yields a mean terminal flow velocity that is significantly below the ideal gas value.

Two-Phase Expansions

As already addressed in the preceding section on the reference state for the enthalpy, supersonic jet expansions from a thermodynamic state where a vapor and a liquid coexist, e.g., as found at the triple point, may yield two quite different terminal flow velocities, matching the two distinct enthalpy changes of the condensed and the noncondensed fraction. As a matter of principle, a well-defined equilibrium state in the stagnation reservoir is indispensable for a meaningful thermodynamic treatment. If, however, the initial perfectly equilibrated state $H_0(P_0, T_0)$ is located just above the binodal in the T – S phase diagram, condensation may occur already within the nozzle itself. Hence, both the vapor and the condensed phase will be accelerated during the jet expansion. In a simplified

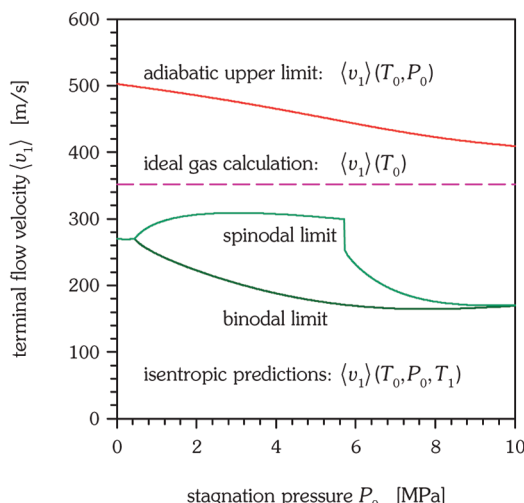


Figure 11. Mean terminal flow velocity $\langle v_1 \rangle$ of a supersonic beam of neon, calculated for a source temperature of $T_0 = 60.0$ K. Depicted are results for the jet expansion of an ideal gas according to eq 5, for the adiabatic jet expansion of the real fluid according to eq 1, using a beam enthalpy of $H_1 = H_1(P_1, T_1)$, and for the isentropic jet expansion of the real fluid to the binodal and the spinodal line according to eq 6.

picture, where the interaction between the two phases is ignored, this coexpansion may yield two distinct peaks in the time-of-flight spectra. These critical stagnation conditions can be substantiated by a calculation of the mean center-of-mass velocity of the working fluid. For any EOS, a Mach number of $M = \langle v \rangle/u$ is obtained at the most constricted point of a converging–diverging nozzle geometry.¹⁶ The Mach number $M = \langle v \rangle/u$ is defined as the ratio of the mean local flow velocity $\langle v \rangle$ to the local velocity of sound, u . Phrased differently, in this simplified model thermodynamic states which yield values of $M \leq 1$ are supposed to be located within the nozzle. Accordingly, Mach numbers exceeding $M = 1$ are expected to belong to the emerging jet. Generalizing eq 1, an expression for the critical enthalpy value H_* is obtained, where $\langle v_* \rangle = u$ applies

$$\langle v_* \rangle = \sqrt{\frac{2(H_0 - H_*)}{N_A m}} \quad (7)$$

The speed of sound can be obtained from the EOS using the relation

$$u^2 = -V^2 \left(\frac{\partial P}{\partial V} \right)_S$$

Hence, for given stagnation conditions, the initial value for the entropy $S_0(P_0, T_0)$ can be computed and used to numerically track the isentropic expansion path, i.e., to calculate both the local sound velocity $u(S_0, T)$ and the local enthalpy $H(S_0, T)$ as a function of the decreasing temperature T of the working fluid. The change in enthalpy $H_0(S_0, T_0) - H(S_0, T)$ then permits estimation of the local flow velocity $\langle v \rangle$ in the nozzle. This approach is visualized in Figure 12 for different source conditions.

With the declining temperature of the working fluid, its speed of sound, u , decreases, too (Figure 12A). Simultaneously, the jet is accelerated, characterized by an increasing mean flow velocity, $\langle v \rangle$ (Figure 12B). At some point in the phase diagram, eq 7 will hold; in Figure 12 this condition of $M = 1$ is indicated

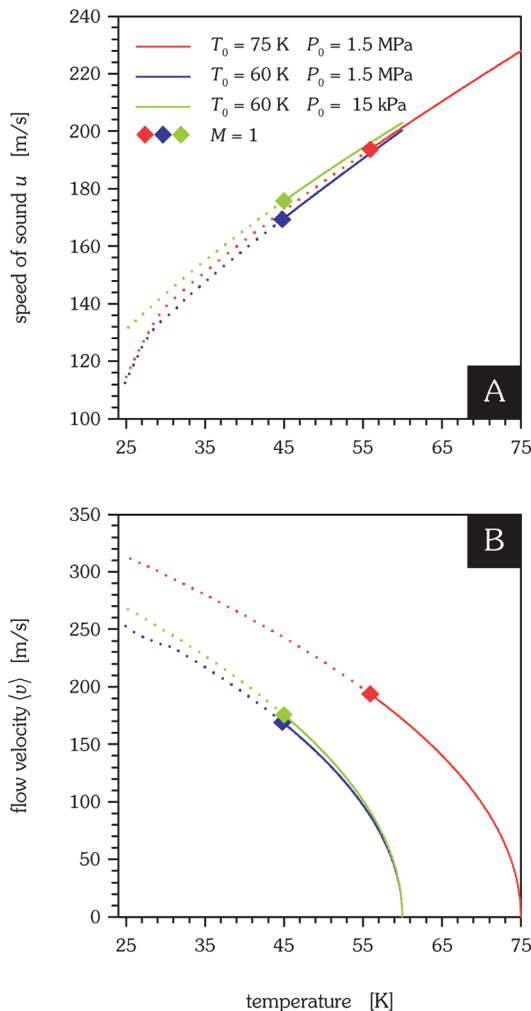


Figure 12. Evolution of the local speed of sound, u (A), and of the mean flow velocity, $\langle v \rangle$ (B), respectively, during the isentropic jet expansion of neon for different source pressures P_0 and temperatures T_0 . The horizontal axis denotes the (decreasing) local temperature, the diamonds mark the position where a Mach number of $M = \langle v \rangle/u = 1$ is attained. Conditions within the valve ($M \leq 1$) are visualized by solid lines.

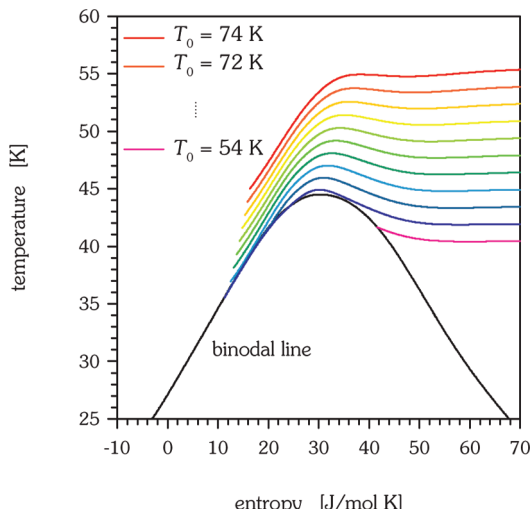


Figure 13. Isentropic jet expansion of Ne, starting from different source temperatures T_0 . Colored lines represent the temperature T_* where a Mach number of $M = 1$ is attained. For $T_0 = 54$ K, a phase separation within the nozzle may occur.

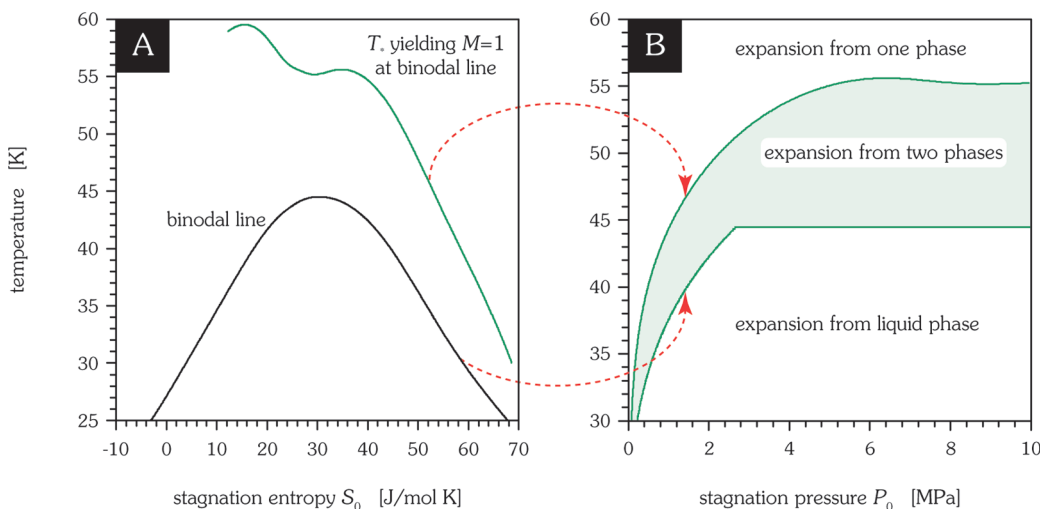


Figure 14. Progression of the “bifurcation” temperature T_* of neon as a function of (A) the stagnation entropy S_0 and (B) the stagnation pressure P_0 . Isentropic jet expansions starting at a source temperature of $T_0 \leq T_*$ will reach the two-phase region already within the nozzle.

by a diamond for the respective expansion isentrope. Figure 13 depicts these states of $M = 1$ for different source temperatures T_0 and stagnation entropies S_0 . As long as all thermodynamic states with $M \leq 1$ are made up of only one aggregation state, it may be assumed that nucleation sets in only during the jet expansion. In this case, both monomers and clusters are supposed to reach the same final flow velocity $\langle v_1 \rangle$ as discussed above. If, on the other hand, the state point where the condition of $M = 1$ holds is already located within the two-phase region, both a condensed and a noncondensed fraction of the working fluid will be expanded simultaneously. Neglecting interactions between the liquid and the vapor phase during the jet expansion two separate peaks with markedly different flow velocities may be anticipated, due to two different stagnation enthalpies $H_v(P_{\text{sat}}, T_{\text{sat}})$ and $H_l(P_{\text{sat}}, T_{\text{sat}})$. The noteworthy exception to this expectation is an isentropic jet expansion passing through the critical point, where $H_l = H_v$. In accord with this reasoning, the separation of the two peak positions is predicted to strongly depend on the stagnation entropy, S_0 .

Starting from the binodal line, it is thus possible to compute the transition source temperature T_* . Isentropic jet expansions starting at a stagnation temperature of $T_0 \leq T_*$ will reach the two-phase region already within the nozzle, as characterized by the Mach number evaluation, and result in a bifurcation of the corresponding velocity distribution. Figure 14 displays this transition temperature T_* for isentropic jet expansions of neon.

Summary

In summary, a consistent thermodynamic description of the mean terminal flow velocity of supersonic molecular beams originating from the isentropic jet expansion of a fluid system into a vacuum has been presented. This model is capable of covering not only expansions of gases, but also of liquids and supercritical fluids; in particular, the vapor–liquid phase boundary or the critical point are treated in a most natural way. Its major prediction is a marked pressure dependence of the flow velocity that can be found even for the rare gases and is caused by cluster formation both in the stagnation reservoir and during the jet expansion. All required thermodynamic parameters can be computed in a straightforward way using the most advanced equations of state, with a typical accuracy of 1% even in the region close to the critical point. These computations permit making a point on the final beam temperature and the amount

of clusters present in the beam, prodigiously valuable information not easily available otherwise. Moreover, the onset of condensation already within the nozzle can result in a bifurcation of the mean terminal flow velocity into two components, as indeed has been observed in experiments.

Acknowledgment. The corresponding author acknowledges valuable discussions with Dr. Eric W. Lemmon from the National Institute of Standards and Technology in Boulder, Colorado, USA. The research described in this article is supported by the German–Israeli Foundation for Scientific Research and Development (GIF Grant I-863-37.5/2005) and the Deutsche Forschungsgemeinschaft under Award CH262/5.

References and Notes

- (1) Knudsen, M. *Ann. Phys.* **1909**, *333*, 75–130.
- (2) Knudsen, M. *Ann. Phys.* **1909**, *333*, 999–1016.
- (3) Dunoyer, L. *Radium* **1911**, *8*, 142–146.
- (4) Stern, O. *Z. Phys.* **1920**, *2*, 49–56.
- (5) Stern, O. *Z. Phys.* **1920**, *3*, 417–421.
- (6) Stern, O. *Z. Phys.* **1926**, *39*, 751–763.
- (7) Knauer, F.; Stern, O. *Z. Phys.* **1926**, *39*, 764–779.
- (8) Kantrowitz, A.; Grey, J. *Rev. Sci. Instrum.* **1951**, *22*, 328–332.
- (9) Becker, E. W.; Bier, K. Z. *Naturforsch., A* **1954**, *9*, 975–986.
- (10) Hagena, O. F. Z. *Ang. Phys.* **1963**, *16*, 183–187.
- (11) *Atomic and Molecular Beam Methods*; Scopes, G., Ed.; Oxford University Press: New York, 1988.
- (12) Pauly, H. *Atom, Molecule, and Cluster Beams*; Springer: New York, 2000.
- (13) *Atomic and Molecular Beams*; Campargue, R., Ed.; Springer: New York, 2001.
- (14) Sanna, G.; Tomassetti, G. *Introduction to Molecular Beams Gas Dynamics*; Imperial College Press: London, 2005.
- (15) Walker, W. J. *Philos. Mag.* **1922**, *43*, 589–593.
- (16) Tsien, H.-S. *J. Math. Phys.* **1946**, *25*, 301–324.
- (17) Sherman, P. M. *AIAA J.* **1971**, *9*, 1628–1630.
- (18) Wegener, P. *P. Acta Mech.* **1975**, *21*, 65–91.
- (19) Bier, K.; Ehrler, F.; Hartz, U.; Kissau, G. *Fortschr. Ingenieurwes.* **1977**, *43*, 175–184.
- (20) Sullivan, D. A. *J. Fluid Eng.* **1981**, *103*, 258–267.
- (21) Leung, J. C.; Epstein, M. *AIChE J.* **1988**, *34*, 1568–1572.
- (22) Bober, W.; Chow, W. L. *J. Fluid Eng.* **1990**, *112*, 455–460.
- (23) Cramer, M. S.; Fry, R. N. *Phys. Fluids A* **1993**, *5*, 1246–1259.
- (24) Pedemonte, L.; Bracco, G.; Tatarek, R. *Phys. Rev. A* **1999**, *59*, 3084–3087.
- (25) Christen, W.; Rademann, K. *Phys. Rev. A* **2008**, *77*, 012702.
- (26) Harinck, J.; Guardone, A.; Colonna, P. *Phys. Fluids* **2009**, *21*, 086101.
- (27) Buchenau, H.; Knuth, E. L.; Northby, J.; Toennies, J. P.; Winkler, C. *J. Chem. Phys.* **1990**, *92*, 6875–6889.

- (28) Scheidemann, A.; Toennies, J. P.; Northby, J. A. *Phys. Rev. Lett.* **1990**, *64*, 1899–1902.
- (29) Harms, J.; Toennies, J. P.; Knuth, E. L. *J. Chem. Phys.* **1997**, *106*, 3348–3357.
- (30) Pedemonte, L.; Tarek, R.; Bracco, G. *Rev. Sci. Instrum.* **2003**, *74*, 4404–4409.
- (31) Knuth, E. L.; Schünemann, F.; Toennies, J. P. *J. Chem. Phys.* **1995**, *102*, 6258–6271.
- (32) Christen, W.; Rademann, K.; Even, U. *J. Chem. Phys.* **2006**, *125*, 174307.
- (33) De Dea, S.; Miller, D. R.; Continetti, R. E. *J. Phys. Chem. A* **2009**, *113*, 388–398.
- (34) Christen, W.; Krause, T.; Rademann, K. *Rev. Sci. Instrum.* **2007**, *78*, 073106.
- (35) Becker, E. W.; Bier, K.; Henkes, W. *Z. Phys.* **1956**, *146*, 333–338.
- (36) Greene, F. T.; Milne, T. A. *J. Chem. Phys.* **1963**, *39*, 3150–3151.
- (37) Leckenby, R. E.; Robbins, E. J.; Trevalion, P. A. *Proc. R. Soc. London, Ser. A* **1964**, *280*, 409–429.
- (38) Golomb, D.; Good, R. E.; Brown, R. F. *J. Chem. Phys.* **1970**, *52*, 1545–1551.
- (39) Milne, T. A.; Vandegrift, A. E.; Greene, F. T. *J. Chem. Phys.* **1970**, *52*, 1552–1560.
- (40) Hagen, O. F.; Obert, W. *J. Chem. Phys.* **1972**, *56*, 1793–1802.
- (41) Golomb, D.; Good, R. E.; Bailey, A. B.; Busby, M. R.; Dawbarn, R. *J. Chem. Phys.* **1972**, *9*, 3844–3852.
- (42) Yealland, R. M.; Deckers, J. M.; Scott, I. D.; Tuori, C. T. *Can. J. Phys.* **1972**, *50*, 2464–2470.
- (43) Knuth, E. L. *J. Chem. Phys.* **1977**, *66*, 3515–3525.
- (44) Hagen, O. F. *Surf. Sci.* **1981**, *106*, 101–116.
- (45) Stein, G. D. *Surf. Sci.* **1985**, *156*, 44–56.
- (46) Hagen, O. F. Z. *Phys. D* **1987**, *4*, 291–299.
- (47) Knuth, E. L. *J. Chem. Phys.* **1997**, *107*, 9125–9132.
- (48) Knuth, E. L.; Henne, U. *J. Chem. Phys.* **1999**, *110*, 2664–2668.
- (49) Anderson, J. B.; Fenn, J. B. *Phys. Fluids* **1965**, *8*, 780–787.
- (50) Hamel, B. B.; Willis, D. R. *Phys. Fluids* **1966**, *9*, 829–841.
- (51) Knuth, E. L.; Fisher, S. S. *J. Chem. Phys.* **1968**, *48*, 1674–1684.
- (52) Toennies, J. P.; Winkelmann, K. *J. Chem. Phys.* **1977**, *66*, 3965–3979.
- (53) Beijerinck, H. C. W.; Verster, N. F. *Physica C* **1981**, *111*, 327–352.
- (54) Beijerinck, H. C. W.; Kaashoek, G. H.; Beijers, J. P. M.; Verheijen, M. J. *Physica C* **1983**, *121*, 425–436.
- (55) Beijerinck, H. C. W.; Van Gerwen, R. J. F.; Kerstel, E. R. T.; Martens, J. F. M.; Van Vliembergen, E. J. W.; Smits, M. R. Th.; Kaashoek, G. H. *Chem. Phys.* **1985**, *96*, 153–173.
- (56) Miller, D. R. In *Atomic and Molecular Beam Methods*; Scoles, G., Ed.; Oxford University Press: New York, 1988.
- (57) Pedemonte, L.; Bracco, G. *J. Chem. Phys.* **2003**, *119*, 1433–1441.
- (58) McCarty, R. D.; Arp, V. D. *Adv. Cryog. Eng.* **1990**, *35*, 1465–1475.
- (59) Katti, R. S.; Jacobsen, R. T.; Stewart, R. B.; Jahangiri, M. *Adv. Cryog. Eng.* **1986**, *31*, 1189–1197.
- (60) Tegeler, Ch.; Span, R.; Wagner, W. *J. Phys. Chem. Ref. Data* **1999**, *28*, 779–850.
- (61) Lemmon, E. W.; Span, R. *J. Chem. Eng. Data* **2006**, *51*, 785–850.
- (62) Smalley, R. E.; Wharton, L.; Levy, D. H. *Acc. Chem. Res.* **1977**, *10*, 139–145.
- (63) McClelland, G. M.; Saenger, K. L.; Valentini, J. J.; Herschbach, D. R. *J. Phys. Chem.* **1979**, *83*, 947–959.
- (64) Abuaf, N.; Anderson, J. B.; Andres, R. P.; Fenn, J. B.; Marsden, D. G. H. *Science* **1967**, *155*, 997–999.
- (65) Anderson, J. B. *Entropie* **1967**, *18*, 33–37.
- (66) Larsen, R. A.; Neoh, S. K.; Herschbach, D. R. *Rev. Sci. Instrum.* **1974**, *45*, 1511–1516.
- (67) Amirav, A.; Even, U.; Jortner, J. *J. Chem. Phys.* **1980**, *51*, 31–42.
- (68) Broyer, M.; Cabaud, B.; Hoareau, A.; Melinon, P.; Rayane, D.; Tribollet, B. *Mol. Phys.* **1987**, *62*, 559–572.
- (69) Becker, E. W.; Henkes, W. Z. *Phys.* **1956**, *146*, 320–332.
- (70) The statistical properties of a system in a thermodynamic equilibrium are given by its partition function, defining its energy relative to its energy at a temperature of $T = 0$. Hence all thermodynamic energies (U, H, \dots) are given only with respect to an a priori unknown reference value.
- (71) Christen, W.; Rademann, K. *Phys. Scr.* **2009**, *80*, 048127.
- (72) Span, R.; Wagner, W.; Lemmon, E. W.; Jacobsen, R. T. *Fluid Phase Equilib.* **2001**, *183–184*, 1–20.
- (73) Lemmon, E. W.; Huber, M. L.; McLinden, M. O. *NIST Standard Reference Database 23: Reference Fluid Thermodynamic and Transport Properties*; National Institute of Standards and Technology: Gaithersburg, MD, 2007.
- (74) Bailey, A. B.; Dawbarn, R.; Busby, M. R. *AIAA J.* **1976**, *14*, 91–92.
- (75) Bruch, L. W.; Schöllkopf, W.; Toennies, J. P. *J. Chem. Phys.* **2002**, *117*, 1544–1566.
- (76) Ekinci, Y.; Knuth, E. L.; Toennies, J. P. *J. Chem. Phys.* **2006**, *125*, 133409.
- (77) Kornilov, O.; Toennies, J. P. *Int. J. Mass Spectrom.* **2009**, *280*, 209–212.
- (78) Farges, J.; de Feraudy, M. F.; Raoulta, B.; Torchet, G. *Surf. Sci.* **1981**, *106*, 95–100.
- (79) Debenedetti, P. G. *Metastable Liquids*; Princeton University Press: Princeton, NJ, 1996.

JP102855M